

Integration of orientation information in amblyopia

Behzad Mansouri ^{a,*}, Harriet A. Allen ^{a,b}, Robert F. Hess ^a,
Steven C. Dakin ^c, Oliver Ehrh ^{a,d}

^a McGill Vision Research Unit, 687 Pine Avenue West, Rm. H4-14, Montreal, Que., Canada H3A 1A1

^b School of Psychology, University of Birmingham, Birmingham B15 2TT, UK

^c Institute of Ophthalmology, University College London, 11-43 Bath St., London EC1V 9EL, UK

^d Department of Ophthalmology, Ludwig Maximilians University, Mathildenstrasse 8, 80336 Muenchen, Germany

Received 17 April 2003; received in revised form 1 March 2004

Abstract

A recent report suggests that amblyopes are deficient in processing local orientation at supra-threshold contrasts. To determine whether amblyopes are also poor at integrating local orientation signals, we assessed performance for an orientation integration task in which the orientations of static signals are integrated across space. Our results show that amblyopic visual systems can integrate local static oriented signals with the same level of efficiency as normal visual systems. Although internal noise was slightly elevated, there was no indication that fewer samples were used to achieve optimal performance. This finding suggests normal integration of local orientation signals in amblyopia.

© 2004 Elsevier Ltd. All rights reserved.

Keywords: Amblyopia; Orientation; Integration

1. Introduction

Our emerging understanding of the underlying neural dysfunction in amblyopia has paralleled, to a great extent, our understanding of normal visual function. Initially, amblyopes were found to be poor at detecting spatially simple targets. This deficiency involves the detection of high spatial frequencies (Gstalder, 1971; Hess & Howell, 1977; Lawwill & Burian, 1966; Levi & Harwerth, 1977). Evidence from animal models suggests that the underlying problem lies in the contrast sensitivity and spatial properties of the high spatial frequency responsive neurons in V1 that receive their input from the amblyopic eye (Crewther & Crewther, 1990; Eggers & Blakemore, 1978; Movshon et al., 1987).

There is reason to suspect that the performance loss in amblyopia is not limited to contrast detection of simple high spatial frequency patterns and that, as a consequence, the neural anomaly is not limited to a subset of neurons in V1. Amblyopes have been shown to be deficient in discrimination tasks involving orientation (Bradley & Skottun, 1984; Caelli, Brettel, Rentschler, & Hiltz, 1983; Demanins, Hess, Williams, & Keeble, 1999; Vandebussche, Vogels, & Orban, 1986), spatial frequency (Hess, Burr, & Campbell, 1980), contrast (Hess, Bradley, & Piotrowski, 1983) and phase (Caelli et al., 1983; Lawden, Hess, & Campbell, 1982; Pass & Levi, 1982; Treutwein, Rentschler, Zetzsche, Scheidler, & Boergen, 1996), in positional judgments for well separated elements where contrast sensitivity does not play a part (Hess & Holliday, 1992), in detection of contrast-defined stimuli (Wong, Levi, & McGraw, 2001) and in tasks involving global vision (Hess, McIlhagga, & Field, 1997; Hess, Wang, Demanins, Wilkinson, & Wilson, 1999; Popple & Levi, 2000) and motion detection

* Corresponding author. Tel.: +1 514 842 1231x35307; fax: +1 514 843 1961.

E-mail address: behzad.mansouri@mail.mcgill.ca (B. Mansouri).

(Simmers, Ledgeway, Hess, & McGraw, 2003). While the above mentioned anomalies suggest a more extensive deficit, our incomplete knowledge of processing sites of these tasks precludes any strong conclusion about whether there is a primary deficient locus in the extra-striate cortex. One exception of this is the global motion task as there is detailed neurophysiological evidence in monkeys and psychophysical evidence in humans that this involves the integration of local V1 motion signals within area MT/MST in extra-striate cortex. The evidence for this comes from single cell recording in extra-striate cortex, where cells have large receptive fields, with sub-units thought to be the basis of such integration (Movshon, Adelson, Gizzi, & Newsome, 1985), and firing patterns that are highly correlated with performance in global motion tasks (Britten, Shadlen, Newsome, & Movshon, 1992; Salzman, Murasugi, Britten, & Newsome, 1992). Furthermore, there is behavioral evidence for an extra-striate basis for this task from both monkeys with target lesions to area MT (Newsome & Pare, 1988) and patients with vascular lesions involving this area who exhibit specific deficits involving motion integration (Baker, Hess, & Zihl, 1991; Rizzo, Nawrot, & Zihl, 1995; Vaina, Lemay, Bienfang, Choi, & Nakayama, 1990; Zihl, von Cramon, & Mai, 1983) but not for detection of local motion (Hess, Baker, & Zihl, 1989). Although a number of deficits have been identified in V1 cells driven by the amblyopic eye of deprived animals (e.g. spatial and orientational tuning, contrast sensitivity, etc.) there have been no reports of V1 motion deficits (Kiorpes, Kiper, O'Keefe, Cavanaugh, & Movshon, 1998). Thus the finding of global motion deficits in amblyopes (Simmers et al., 2003) suggests that the amblyopic deficit may involve integrative functions known to occur beyond V1. Simmers et al. (2003), relying on an accepted 2-stage model of global motion processing (Morrone, Burr, & Vaina, 1995) in which the first stage is contrast sensitive and identified with V1 processing and the second stage is purely integrative and identified with extra-striate processing (e.g. area MT/MST), delineate both components of the overall motion deficit for global stimuli. They isolate a significant deficit that involves the integration of local motion signals, implicating the extra-striate cortex. Having ruled out any contribution from, the reduced contrast sensitivity exhibited by cells in V1, the only other possible V1 influence could be from positional uncertainty, if its site were to be in V1. Such an influence is unlikely in a task where the element positions are stochastic unless it contributes, in some way, to a deficit to the processing of local motion. Such a proposal has neither psychophysical (Hess & Anderson, 1993) nor neurophysiological (Kiorpes et al., 1998) support. Furthermore, Simmers et al. (2003) show that the fellow fixing eye is also deficient at global motion detection and that this is also confined to the integrative

aspect of the task, implicating a site in the pathway where the majority of cells are binocular. Recently, Simmers, Ledgeway, and Hess (forthcoming) has shown, using an equivalent global form task, that this extra-striate deficit in amblyopia also affects the ventral stream.

In order to ascertain whether this global motion deficit is a reflection of a more general inability to integrate visual information across space, we examined the efficiency with which the amblyopic visual system can integrate visual information of a purely spatial character. We chose orientation not only because of its importance in early visual processing but also because it has recently been suggested that global orientation processing of supra-threshold stimuli is specifically disrupted in amblyopia (Barrett, Pacey, Bradley, Thibos, & Morrill, 2003; Popple & Levi, 2000). We chose a paradigm where integrative performance did not depend on the spatial distribution of the elements whose orientation signals were to be integrated. This factored out any contribution from the, already known, elevated positional uncertainty in amblyopia (Hess & Holliday, 1992; Levi & Klein, 1985) allowing us to measure unambiguously the integrative performance of amblyopic eyes for local, oriented, stimuli of supra-threshold contrast.

The equivalent noise approach has been applied in a number of vision studies before e.g. contrast sensitivity (Ahumada & Watson, 1985; Pardhan, 2004), luminance offset detection (Barlow, 1957), coding of spatial position (Watt & Hess, 1987; Zeevi & Mangoubi, 1984), discrimination of edge blur (Watt & Morgan, 1983), spatial frequency acuity (Heeley, 1987), contour integration (Hess & Dakin, 1999), and orientation discrimination (Heeley, Buchanan-Smith, Cromwell, & Wright, 1997).

Previously, Dakin (2001) used this task and showed that normal observers can integrate local orientation information efficiently over a large range of stimulus sizes, numerosity and density. His results were well described by the equivalent noise model. Given that thresholds are estimates of response variance, the non-ideal behavior of observers with noiseless stimuli (zero orientation variance) can be expressed as an additive, internal noise, which means that in no variance condition, the visual system behaves as if it is performing the task in the presence of a certain amount of variability in the stimulus population. The level of internal noise can be simply measured by increasing the amount of external noise in the stimulus and determining the point at which observer's performance begins to deteriorate. The observer's robustness to increasing amounts of external noise will depend decreasingly on internal noise and increasingly on how many samples are averaged over because more samples gives a better average estimate from the stimuli population which decreases the effect of the external noise. The form of the equivalent noise model is:

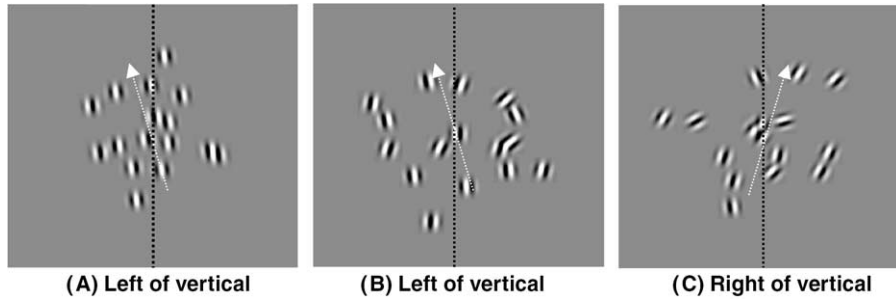


Fig. 1. *Stimuli*. Arrays of 16 randomly placed, oriented Gabor elements with mean orientation (indicated by the arrow for illustrative purposes only, not present during testing) relative to the vertical (indicated by the dashed lines for illustrative purposes only, not present during testing). Each Gabor is a sample from a Gaussian distribution of orientations with a mean equal to the cued orientation and a variable bandwidth. In this figure we show example stimuli for three different standard deviations of the parent orientation distribution; a standard deviation of 0° (A), 16° (B), and 28° (C).

$$\sigma_{\text{obs}} = \sqrt{\sigma_{\text{int}}^2 + \frac{\sigma_{\text{ext}}^2}{n}}$$

where σ_{obs} is the observed threshold, σ_{ext} is the external noise, σ_{int} is the estimated equivalent intrinsic or internal noise and n is the estimated number of samples being employed. In terms of the orientation discrimination task, σ_{obs} corresponds to the threshold for orientation discrimination, σ_{ext} to the standard deviation of the distribution from which the samples are derived (see Section 2), σ_{int} to the noise associated with the measurement of each orientation sample and their combination and n corresponds to the estimated number of orientation samples being combined by the visual system.

Assumptions underlying equivalent noise:

(1) Orientation integration involves averaging. Efficiency on our tasks indicates that observers invariably employ more than one sample, i.e. they are combining information across space and are not relying on a single element to perform the task. This does not mean observers necessarily use the average (although this would be optimal); other strategies, such as using a peak in the orientation statistics, might also suffice. However, by employing textures composed of orientation drawn from skewed distributions Dakin and Watt (1994) were able to show that observers' performance was consistent with their using the average orientation and not the peak.

(2) Nature of the noise. Equivalent noise assumes that performance is limited by additive and multiplicative noise. Additive noise is due to noise on the detectors registering local orientation and could, for example, be plausibly linked to the finite orientation bandwidth of cells in V1. Sampling efficiency is equivalent to a global multiplicative noise source; i.e. one that increases with the strength of signal being pooled. Multiplicative noise is a ubiquitous feature of neural systems and has been observed in neurons responsible for integration along other stimulus dimensions, e.g. motion; MT neurons (Britten, Shadlen, Newsome, & Movshon, 1993).

(3) Constant internal noise. The two parameters of internal noise and sampling efficiency in the standard equivalent noise function are fixed across all levels of external noise. This assumption is made on the grounds of parsimony; we do not need to change noise levels as a function of stimulus variance to account for our data.

In the main experiment, observers viewed an array of 16 randomly positioned, oriented Gabors that were samples from an orientation distribution whose standard deviation was varied. The task was to determine whether the mean orientation of the array was clockwise or counterclockwise (see Fig. 1) from vertical. The results were fitted by the equivalent noise model, described above, to derive the measures of internal noise and number of samples. To ensure that any differences between these measures for normal and amblyopic observers were due solely to integrative function, we equated performance for a single Gabor element for a similar orientation task. This ensured that performance was equated for this task for an individual element and that therefore any difference in the derived measures must be the results of integration per se.

2. Methods

2.1. Observers

Ten normal and twelve amblyopic observers were recruited for this experiment. Two of the normal observers were the authors. The others were naïve to the purpose of experiment. All observers were optically corrected if necessary. Clinical details of amblyopic observers are presented in Table 1. Eye dominance in normal observers was assessed for each subject using a sighting test (Rosenbach, 1903).

2.2. Stimuli

The stimuli were arrays of Gabor micro-patterns presented on a mid-gray background. The envelope of the

Table 1
Clinical details of the amblyopic observers participating in the experiment

Observers	Age	Type	Refraction		Acuity	Strabismus	History, stereo
AM	31 yr	RE Strab	-3.75 DS -3.25 DS		20/50 20/25	ET + 3°	Detected age 3 yr, patching for 3 yr
LN	49 yr	RE Strab	+3.75–3.75 +3.00–2.00	120° 80°	20/30 20/20	ET + 10°	Detected age 3 yr, glasses since, patching 6w, strabismus surgery RE age 20 yr
MA	22 yr	LE Aniso	-0.25 DS +3.50–0.50	0°	20/15 20/200	Ortho	Detected age 3 yr, patching for 4 yr, glasses for 8 yr
MG	28 yr	RE Strab	-0.50 DS +0.50 DS		20/100 20/15	ET + 1°	Detected age 4 yr, patching for 6 months, no surgery
MM	27 yr	LE Aniso	+0.25–1.75 +0.75–3.50	135° 55°	20/20 20/30	Ortho	Detected age 6 yr, 6 months patching basic stereovision present
NG	30 yr	RE Mixed	+5.00–2.00 +3.50–1.00	120° 75°	20/70 20/20	ET + 8°	Detected age 5 yr, patching for 3 months, no glasses tolerated, 2 strabismus surgery RE age 10–12 yr
RB	49 yr	LE Aniso	+3.25 DS +4.75–0.75	45°	20/15 20/40	XT - 5°	Detected age 6 yr, glasses since 6 yr, no other therapy, near normal local stereo vision
VL	35 yr	LE Aniso	+0.50 DS +3.50–3.00	50°	20/20 20/50	Ortho	Detected age 6 yr, ϕ
YC	31 yr	LE Strab	+2.00 DS +2.00 DS		20/15 20/40	ET + 10°	Detected age 2 yr, patching for 4 yr, glasses for 16 yr
BB	58 yr	LE Strab	+0.50–0.50 +1.25–0.25		20/15 20/600	ET + 5°	Detected age 8 yr, surgery to correct angle of large eso, patching for 6 months
AT	21 yr	LE Aniso	+0.50 DS +0.50–2.0	200°	20/15 20/30	Ortho	Detected age 3 yr, glasses since 8 yr no other therapy
PH	33 yr	LE Strab	-2.0+0.50 DS +0.50 DS		20/25 20/63	ET + 5°	Detected age 4 yr, patching for 6 months, surgery when he was 5 yr

The following abbreviations have been used; strab for strabismus, aniso for anisometropic, RE for right eye, LE for left eye, ET for esotropia, XT for exotropia, ortho for orthotropic alignment, sph for dioptre sphere.

Gabor had a standard deviation of 0.4° . The spatial frequency of sinusoidal modulation within the Gabor was varied between 0.52 cycles per degree (cpd) and 4.16 (cpd) depending on the experiment. Gray levels of patches were added when they overlapped and clipped appropriately at the maximum or minimum gray level when they were outside the range of the screen, although this only happened rarely. The Gabors were randomly distributed in a circular area, which varied between 3° and 12° wide. The center of the distribution was the center of the screen. The orientation in each Gabor micro-pattern was selected from a Gaussian distribution with a mean equal to the cued orientation, i.e. $90^\circ \pm$ the cue generated by APE, an adaptive method of constant stimuli (Watt & Andrews, 1981) and a variable bandwidth. The distribution's standard deviation, σ , was varied from 0° (all elements aligned) to 28° (high orientation variability) as shown in Fig. 1. The dotted lines and arrows in Fig. 1 represents the notional vertical and mean orientation of the array.

2.3. Apparatus

An Apple Macintosh G3 computer was utilized in the experiment. The Matlab environment (MathWorks Ltd.) and Psychophysics ToolBox (Brainard, 1997) were used for programming. All stimuli were displayed on a 20 in. Sony monitor (Trinitron 520GS), which was calibrated and linearized using Graseby S370 photometer and the Video Toolbox (Pelli, 1997) package. Pseudo 12 bit contrast accuracy was achieved by using a video attenuator (Pelli & Zhang, 1991), which combined the RGB outputs of the graphic card (ATI Rage 128) into the G gun. The monitor had a refresh rate of 75 Hz. The mean luminance of the screen was 33 cd/m^2 and the resolution was 1152×870 pixels. One pixel on the screen was 0.32 mm, which was $2.12'$ of the observers' visual angle from the viewing distance of 52 cm. The observers performed the task monocularly beginning with the fellow fixing eye (in amblyopes) and dominant eye (in normals), with the other eye patched.

2.4. Psychophysics

(A) Equating orientation discrimination performance for isolated stimuli: in order to equate the performance levels for this task for an individual Gabor stimulus for fellow fixing and amblyopic eyes, we measured the orientation discrimination threshold for a single Gabor, of the exact type used in the later integration experiment, as a function of the contrast of the Gabor. This single Gabor was presented in a random position within the 6° stimulus area and was tilted clockwise or counterclockwise from vertical. The magnitude of the tilt was determined by the APE procedure. A single temporal interval two alternative forced choice paradigm was used. Observers had to judge whether the patch was rotated clockwise or counterclockwise (tilted to right or left of vertical). The observers' orientation threshold was estimated as the slope of the best fitting cumulative Gaussian psychometric function derived from between 192 and 340 presentations. 95% confidence intervals were estimated from 1000 bootstrap replications of the fit (Foster & Bishop, 1987). Fig. 2 shows orientation discrimination thresholds for 1 Gabor from normal and amblyopic observers.

In the amblyopic observers, the single Gabor was presented to the amblyopic eye with a fixed, high, contrast (75%) and to the fellow fixing eye with a range of contrasts. The threshold for the fellow fixing eye increased with decreasing contrast (see Fig. 2B). Therefore the contrast with which the fellow fixing eye gave an equal threshold for orientation discrimination to that of the amblyopic eye (with 75% contrast stimuli) was selected. In the subsequent integration experiment the stimuli were presented with the adjusted contrasts for the fellow fixing eyes and 75% contrast for the amblyopic eyes. This task was performed with all amblyopic observers with stimuli of all tested spatial frequencies in order to find the matching contrast for the fellow fixing eye of each observer in each condition.

For our group of normal controls we used stimuli of 25% contrast in the integration experiments. This contrast represents the average contrast level used for the fellow fixing eyes of amblyopes.

(B) Orientation integration: Arrays of randomly positioned, oriented Gabors were presented. The orientation of an individual array element was chosen from a Gaussian distribution. A single temporal interval two alternative forced choice paradigm was used. The observers' task was to judge whether the mean orientation of the array of Gabors was rotated clockwise or counter clockwise (tilted to right or left of vertical) (see Fig. 1). In the main experiment, the stimuli were shown for 500 ms although this was varied (13–500 ms) in a later experiment. Orientation discrimination thresholds were obtained from between 192 and 340 presentations for each of a number of standard deviations of the parent

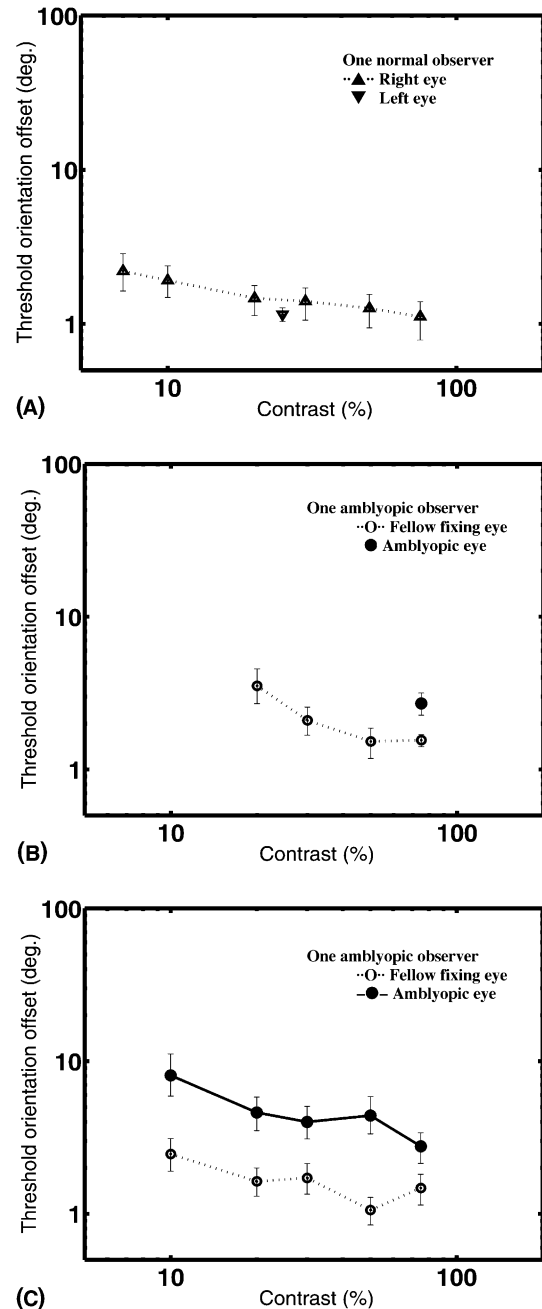


Fig. 2. Equating performance for single elements. Orientation discrimination thresholds measured as a function of contrast for a single Gabor element. In (A), results are shown for a normal observer. In (B), results are shown for an amblyope (AM) in which the performance of the amblyopic eye is fixed at a high contrast (75%) and the performance of the fellow fixing eye is measured as a function of contrast. In this case to equate performance for the amblyopic eye viewing a 75% contrast stimulus, we would need to use a 25% contrast stimulus viewed by the fellow fixing eye. In (C), results are shown for the amblyopic and fellow fixing eyes of an amblyope (BB) as a function of contrast. With lower contrast, there is worse orientation discrimination performance. Error bars: 95% confidence intervals (CIs).

distribution i.e. external noise (10 levels typically between 0° and 28°). The orientation threshold for each level of variability of the parent distribution was

estimated as the slope of the best fitting cumulative Gaussian function using a maximum likelihood procedure. The model described in the introduction was fitted to the thresholds separately for each eye of each observer in each condition.

2.5. Statistics

We tested the parameters from our equivalent noise model, internal noise and number of samples separately. In order to compare the differences between the groups, we used a 2 (between) \times 2 (within) \times 3 (within) analysis of variance (ANOVA) for the variables of observer (normal and amblyopic), eye (amblyopic and fellow fixing in amblyopic observers and dominant and non-dominant in normal observers) and spatial frequency (low, medium and high). We also calculated 95% confidence intervals for the thresholds from each individual psychometric function and used it to compare individual sets of data within the groups.

3. Experimental manipulations

3.1. Integration within different spatial frequency bands

In the first experiment low spatial frequency stimuli (0.52 cpd), which were well within the acuity limit of all observers, were tested in 10 amblyopic and 10 normal observers. In each trial, 16 micro-patterns were presented within the stimulus area (see Fig. 1). The stimulus area was 6° of visual angle. The exposure duration time was 500 ms.

Since contrast sensitivity is similar to normal in the majority of amblyopes for low spatial frequencies (Hess & Howell, 1977), these stimuli are useful to compare the integration function of the amblyopic and normal eyes with a stimulus for which contrast thresholds are normal or only minimally affected.

In order to better understand the influences of different spatial frequencies on orientation integration for the amblyopic visual system, 6 amblyopic (AM, LN, MA, MG, MM and RB, see Table 1) and 6 normal observers were tested with medium and high spatial frequency Gabor arrays. The spatial frequency of the high frequency stimulus was a factor of 2 below the highest spatial frequency that the observers reported that they could see—except in the (MA) case where this led to a very high orientation discrimination threshold (87°), so the spatial frequency was reduced by a further factor of 2. The average high spatial frequency stimuli were about a factor of 6–8 (3.12–4.16 cpd) above the low frequency stimuli (0.52 cpd). These were stimuli for which contrast thresholds were elevated in amblyopic eyes. The medium frequency stimuli typically were between the high and low spatial frequencies (e.g. 2 cpd).

3.2. Exposure duration

While some studies have argued that amblyopic visual system is more detrimentally affected by decreasing the exposure duration than the normal visual system (Rentschler & Hilz, 1985; Weiss, Rentschler, & Caelli, 1985), others have shown very little effect of decreasing exposure duration (Demanins & Hess, 1996a; Loshin & Jones, 1982). The discrepancy may be due to the different tasks studied, in the former case it was vernier acuity and phase discrimination, whereas in the latter it was contrast thresholds and positional sensitivity for well separated stimuli. To ascertain whether exposure duration is important for local orientation integration in amblyopia, we measured integration performance for a range of exposure durations, between 13 ms and 500 ms. This was done in one normal and five amblyopic observers (MA, PH, RB, MM and BB).

3.3. Numerosity, density and stimulus extent

It has been previously shown in normal observers (Dakin, 2001) that the number of presented elements relates strongly to the sampling efficiency of an observer and the internal noise can be affected by the density of the element array. To better understand the mechanisms involved in integration by the amblyopic visual system, we varied these parameters in one normal and five amblyopic observers (MA, AT, PH, RB and MM).

Three parameters were varied in this experiment; number, density of elements and radius of stimulus area. Since these parameters are inter-related, changing one without changing the others is not possible. Therefore to study the effects of these parameters individually, one variable was kept fixed at a time, whilst allowing the other two to co-vary. In the first condition, radius of stimulus area was held constant (6°) and the number of elements (16, 64 and 256) and the density (0.176, 0.705 and 2.820 element/cm²) co-varied. In the second condition, the number of elements was held constant (64) and the radius of stimulus area (3°, 6° and 12°) and the density (2.820, 0.705 and 0.176 element/cm²) co-varied. In the third condition, the density was held constant (0.705 element/cm²) and the radius of stimulus area (3°, 6° and 12°) and the number of elements (16, 64 and 256) co-varied. In all conditions, the presentation time was 500 ms.

4. Results

4.1. Equating orientation performance levels

Fig. 2A shows the relationship between the orientation discrimination threshold for a single Gabor and contrast for a normal observer. Performance is relatively

constant at high contrasts but deteriorates as the contrast is reduced (Hess, Ledgeway, & Dakin, 2000). Similar threshold performance at one contrast level is seen for the non-dominant eye (inverted triangle) of this normal observer. In Fig. 2B an example is shown of data equating the performance levels between fellow fixing and amblyopic eyes of our amblyopic observers. The filled symbol represents the orientation discrimination performance of the amblyopic eye for a fixed 75% contrast stimulus. The open symbols and dotted curve represent the performance of the fellow fixing eye as a function of stimulus contrast. In this case, to equate performance levels for the single element, the contrast of the stimuli for the fellow fixing eye needs to be reduced to a third (i.e. 25%) of that seen by the amblyopic eye. We repeated these measurements for all amblyopic observers and used the appropriate contrast for the fellow fixing eye that equated orientation discrimination performance for 75% contrast stimuli seen by the amblyopic eye. In Fig. 2C, we show how the amblyopic eyes' performance (filled symbols and solid curve) changes with reducing the contrast below 75%. It exhibits a stronger dependence on contrast than that seen for the fellow fixing eye (unfilled symbols and dotted curve) which was expected due to the known poor performance for orientation discrimination for amblyopic observers when using low contrast stimuli (Demany et al., 1999).

Averaged results for the orientation discrimination of an isolated Gabor are shown in Fig. 3A for fellow fixing eyes at two contrast levels and amblyopic eyes for the three spatial frequencies tested. At the same physical contrast, the amblyopic eye exhibits poorer orientation discrimination compared with the fellow fixing eye ($p < 0.05$) although the magnitude of this effect is only large at high spatial frequencies. When the contrast of the fellow fixing eye is reduced to around 20% there was no statistically significant difference between the performance of the fellow fixing and amblyopic eyes.

4.2. Integrating local oriented signals

The results shown in Fig. 3B represent a similar comparison to that in 3A for an array of identically oriented Gabors. Here we compared mean orientation performance for the amblyopic (75% contrast) and fellow fixing eyes (adjusted contrast) and the normal eyes of non-amblyopic observers (25% contrast). There is no statistically significant difference between the means of these three conditions indicating that our method of equating performance between the amblyopic eyes, fellow fixing, and normal eyes was successful. Notice that the orientation thresholds for the high spatial frequency Gabors are much reduced in the multiple element, compared with the isolated element, condition. It would seem that the reduced orientation discrimination performance for isolated high spatial frequency Gabors (Fig. 3A) may

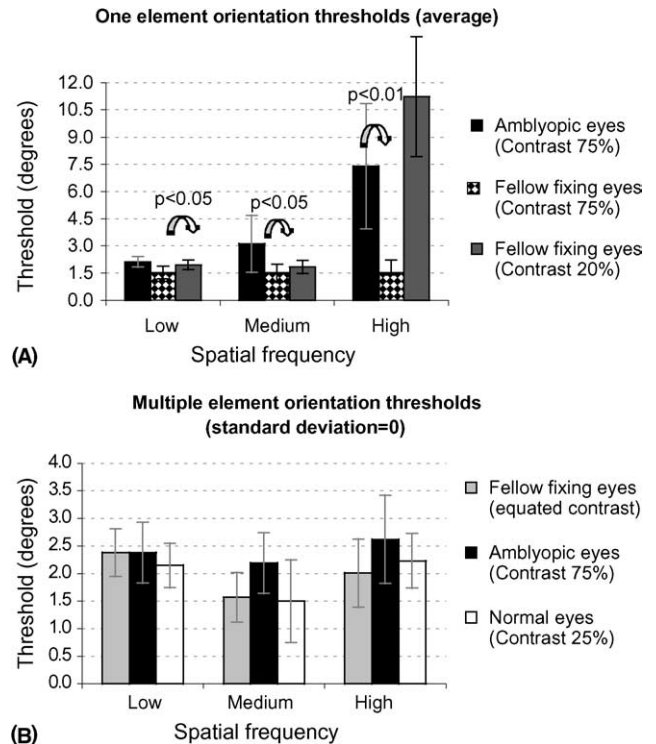


Fig. 3. (A) *One element orientation threshold in amblyopic observers.* Comparison of mean one element discrimination threshold of amblyopic eyes (contrast 75%) (filled bars), fellow fixing eyes (contrast 75%) (dotted bars) and fellow fixing eyes (contrast 20%) (gray bars) for tested spatial frequencies are presented. Error bars represent ± 0.5 SD. There are significant differences in discrimination thresholds between the amblyopic and fellow fixing eyes ($p < 0.05$), which are more prominent with stimuli with high spatial frequency ($p < 0.01$). Decreasing the contrast of the stimuli to 20% for the fellow fixing eyes increased the mean threshold, especially in high spatial frequency condition. (B) *Multi element orientation thresholds.* The average threshold from the amblyopic eyes (filled bars) and fellow fixing eyes (gray bars) and average of the dominant and non-dominant eyes of normal observers (open bars) are compared for all tested spatial frequencies when all the 16 stimuli are aligned ($SD = 0$). Error bars represent ± 0.5 SD. In all spatial frequency conditions the thresholds of the amblyopic, fellow fixing and normal eyes are not significantly different ($p > 0.05$). Also, there is no significant difference between the various spatial frequencies ($p > 0.05$).

be due to either an inability to detect some stimuli when their position is uncertain or to the benefit of being able to integrate a number of identical individual signals.

Our next step was to compare performance for the mean orientation task when the individual Gabor elements within the array did not have identical orientations. As illustrated in Fig. 1 we introduced orientational variability into the display by having the orientation of each Gabor element be a sample from a parent Gaussian orientation distribution whose mean was at the vertical \pm the cued orientation. We measured the threshold orientation offset required to reach criterion performance on this mean orientation task as a function of the standard deviation of the distribution from which the individual orientation samples were

drawn. Example results of a normal observer (A) and an amblyopic observer (B) are displayed in Fig. 4. The discrimination threshold for judging the mean orientation of an array of 16 randomly positioned Gabors is plotted against the standard deviation of the orientation distribution. The error bars represent 95% confidence intervals obtained from our bootstrapping procedure. The curves represent the equivalent noise model described in the introduction fitted to the orientation thresholds with the best fit estimates for internal noise (IN) and number of samples (NS) values shown in the inset. In the case of the normal observer (Fig. 4A), performance of the right (dominant—open symbols and dotted curve) and left (non-dominant—filled symbols and solid curve) eyes are consistent with approximately 6.2 and 5.0 out of the 16 available samples being used to estimate the mean

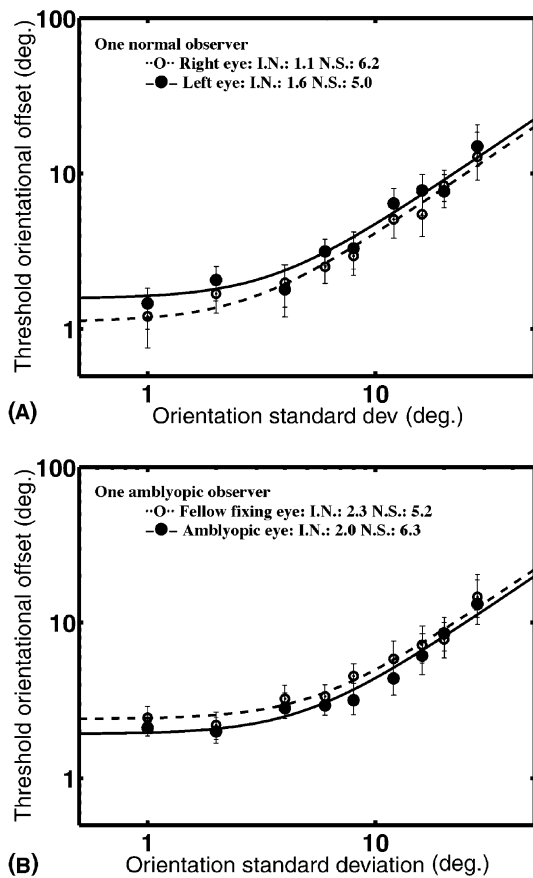


Fig. 4. Mean orientation thresholds. Orientation discrimination thresholds are plotted against the standard deviation of the orientation distribution from which the samples were taken. In this case, 16 Gabors comprised the stimulus array. The curve is the best fit for the equivalent noise model. The error bars represent 95% confidence intervals. The parameters of this fit, internal noise (IN) and number of samples (NS) are shown in the inset. In (A), results are shown for dominant (open symbols and dotted curve) and non-dominant (filled symbols and solid curve) eyes of a normal observer (HA) whereas in (B), results are shown for the amblyopic (filled symbols and solid curve) and fellow fixing (open symbols and dotted curve) eyes of a strabismic amblyopic (MA).

orientation of the Gabor array, respectively. The estimate of internal noise was 1.1° and 1.6°. The results in Fig. 4B compare performance for the fellow fixing (open symbols and dotted curve) and amblyopic eyes (filled symbols and solid curve) of one of our amblyopic observers (RA). This is a typical result showing similar performance with the fellow fixing and amblyopic eyes of this individual. The internal noise and number of samples in the amblyopic eye (2.0° and 6.3°) were not significantly different from those of the fellow fixing eye (2.3° compared with 5.2°).

4.3. Integration for different spatial frequencies

In Fig. 5 we show results in a similar form to that described above but averaged over the eyes of our normal and amblyopic observers. In each case, we plot

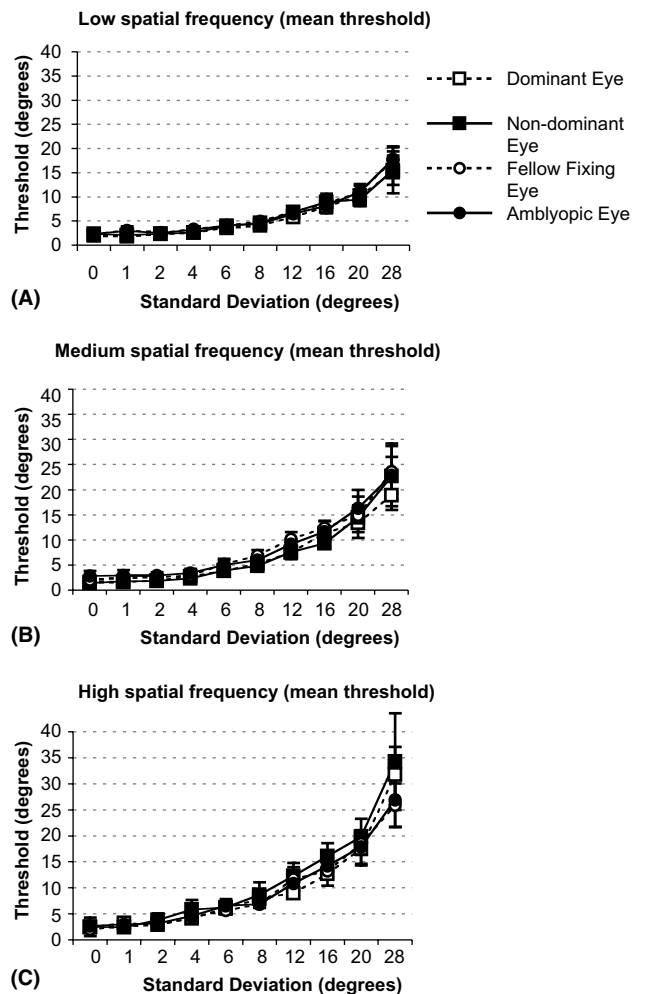


Fig. 5. Average mean orientation thresholds. Averaged thresholds are displayed for the amblyopic (filled circles and solid lines) eyes, the fellow fixing eyes (open circles and dotted curve) and eyes of normal observers (open and filled square symbols correspond to dominant and non dominant eyes, respectively) for stimuli of low (A), medium (B) and high (C) spatial frequency. The error bars represent ± 0.5 SD.

the averaged thresholds for each eye of our normal observers (dominant and non-dominant eyes) and for each eye of our amblyopes (fellow fixing and amblyopic). The error bars represent ± 0.5 standard deviation (SD) of the population. We did not find any significant differences between the thresholds from normal and amblyopic eyes. This was true for all low (Fig. 5A), medium (Fig. 5B) and high (Fig. 5C) spatial frequencies.

From each individual result we derived the best fits for the parameters of internal noise and number of samples and averaged these individually derived measures across our observer populations. These measures are shown for the three populations, normals (average threshold of both eyes of normal observers), fellow fixing eyes and amblyopic eyes (of amblyopic observers) in Fig. 6. For the purpose of clarity, the error bars represent ± 0.5 SD. The internal noise parameter was significantly higher at high spatial frequencies (fellow fixing versus amblyopic eye only, $p < 0.05$), however at low and medium spatial frequencies, internal noise was not significantly different for amblyopic eyes ($p > 0.05$). In terms of the number of samples parameter (Fig. 6B),

as the spatial frequency increased, the number of samples taken by the visual systems decreased, regardless of being amblyopic or non-amblyopic ($p < 0.05$ for medium versus high spatial frequency and $p < 0.01$ for low versus high spatial frequency). There was no significant difference between the number of samples taken by the amblyopic and non-amblyopic eyes ($p > 0.05$).

For the purpose of clarity, the internal noise and number of samples values in each individual amblyopic (Table 2(panels A and B), respectively) and normal observer (Table 2(panels C and D), respectively) are presented.

4.4. Exposure duration

The previous results were obtained at an exposure duration of 500 ms. In Fig. 7A we show the effect of two presentation durations, 500 ms versus 100 ms on orientation discrimination performance on our single element task for one of our amblyopic observers (BB). Short stimulus durations disadvantage the performance of the amblyopic eye relative to its fellow fixing eye and therefore a lower contrast is required for the fellow fixing eye to equate the orientation performance of the fellow fixing and amblyopic eyes. However, once performance for the single element has been equated, the subsequent integration of oriented signals is not significantly different ($p > 0.05$) for fellow fixing and amblyopic eyes (Fig. 7B). Internal noise and number of samples for five amblyopic observers are presented in Table 3.

For completeness we found that integration of orientation information was quite similar across a wide range (500–13 ms) of exposure durations in normal vision (Fig. 7C).

4.5. Numerosity, density and stimulus extent

In our main experiment we used arrays of 16 Gabors, randomly distributed within an area with radius of 6° , giving a density of 0.705 element/cm². We wondered to what extent this initial choice of parameters affected our conclusions. To test this, we varied the numerosity, density and stimulus extent of the oriented Gabors for our integration task with stimuli of the low spatial frequency and compared results for the eyes of one normal (BM) and five amblyopic observers (MA, AT, RA, PH and MM), which are displayed in Fig. 8 (the error bars represent 95% confidence intervals). The results from all of these conditions showed similar patterns of increasing or decreasing internal noise and number of samples for all dominant fellow fixing eyes (open symbols and dashed lines) and non-dominant and amblyopic eyes (filled symbols and solid lines). Furthermore, in almost all of the variable levels, there were no significant differences between the values of internal noise and number

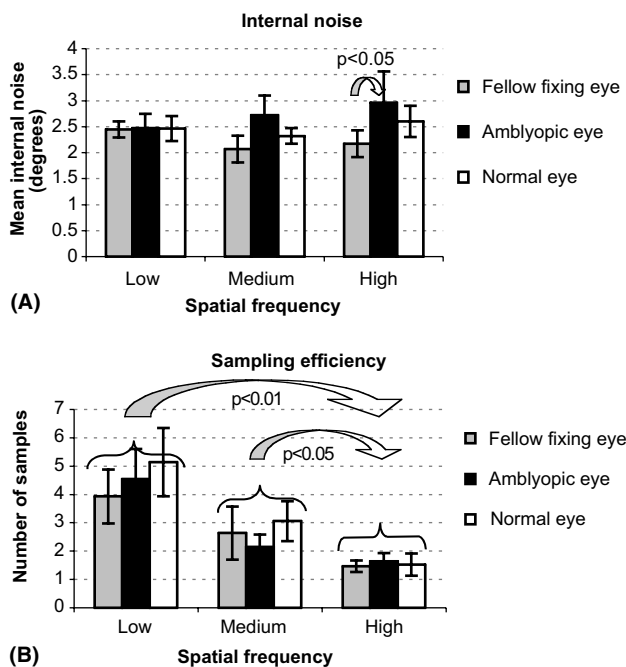


Fig. 6. Internal noise and number of samples. Comparison of the average of the individual estimates of internal noise (A) and number of samples (B) from our model fits for the three variables of, fellow fixing eyes (gray bars), amblyopic eyes (filled bars), and eyes of normal observers (open bars). The error bars represent ± 0.5 SD. In (A), there is significantly higher internal noise for amblyopic eyes compared with either normal eyes or fellow fixing eyes only at high spatial frequency condition ($p < 0.05$). For the number of samples measured in (B), we found no significant different between amblyopic and either normal eyes or fellow fixing eyes, although the number of samples, unlike the internal noise, did show a significant overall reduction with increasing spatial frequency ($p < 0.05$).

Table 2
Internal noise and number of samples in the amblyopic and normal observers

Observers	LSF FFE	LSF AME	MSF FFE	MSF AME	HSF FFE	HSF AME
<i>Panel A</i>						
AM	1.43	1.54	0.27	0.87	0.56	0.98
LN	2.35	1.51	0.96	1.14	1.36	2.24
MA	2.39	1.58	1.38	2.37	3.61	3.78
MG	4.43	5.24	3.75	4.83	4.18	6.78
MM	1.51	1.50	1.16	1.34	1.41	2.07
NG	2.76	2.41	N/A	N/A	N/A	N/A
RB	2.49	2.96	2.35	2.67	1.92	1.93
VL	2.51	2.29	N/A	N/A	N/A	N/A
YC	1.78	1.33	N/A	N/A	N/A	N/A
BB	4.08	5.87	N/A	N/A	N/A	N/A
AT	3.79	5.58	N/A	N/A	N/A	N/A
PH	1.82	2.36	N/A	N/A	N/A	N/A
<i>Panel B</i>						
AM	5.44	6.58	6.55	2.84	1.16	2.14
LN	3.89	3.07	2.00	2.81	1.20	2.06
MA	5.21	6.24	1.87	3.03	2.01	0.79
MG	2.46	3.49	1.89	1.74	1.87	2.17
MM	2.89	3.47	1.60	2.47	1.12	1.43
NG	2.54	4.52	N/A	N/A	N/A	N/A
RB	1.79	2.26	1.25	1.36	1.36	1.24
VL	4.10	8.69	N/A	N/A	N/A	N/A
YC	8.15	5.08	N/A	N/A	N/A	N/A
BB	1.50	0.75	N/A	N/A	N/A	N/A
AT	3.41	4.26	N/A	N/A	N/A	N/A
PH	5.43	5.61	N/A	N/A	N/A	N/A
<i>Panel C</i>						
BM	1.1	1.57	0.72	0.96	1.34	2.09
HA	2.32	2.68	2.07	1.74	3.69	2.00
LA	1.63	1.77	1.25	0.99	1.17	1.80
EK	1.65	1.57	1.03	0.98	1.76	1.82
SD	2.32	2.24	2.39	2.12	3.38	6.77
MA	1.43	1.51	1.31	1.21	2.78	2.66
OE	2.27	1.83	N/A	N/A	N/A	N/A
MM	2.04	1.87	N/A	N/A	N/A	N/A
CH	3.12	3.54	N/A	N/A	N/A	N/A
PA	1.42	1.83	N/A	N/A	N/A	N/A
<i>Panel D</i>						
BM	6.24	4.96	3.82	5.24	1.92	1.65
HA	4.77	5.24	2.42	2.92	0.77	1.24
LA	2.95	1.60	1.42	1.58	1.28	1.83
EK	5.25	5.60	3.10	2.88	2.75	2.75
SD	1.80	1.97	1.68	1.71	1.01	0.49
MA	4.91	4.95	4.95	5.05	2.17	0.55
OE	5.18	4.27	N/A	N/A	N/A	N/A
MM	6.67	10.37	N/A	N/A	N/A	N/A
CH	3.18	4.73	N/A	N/A	N/A	N/A
PA	10.74	7.49	N/A	N/A	N/A	N/A

Panel A: internal noise in amblyopic observers; panel B: number of samples in amblyopic observers; panel C: internal noise in normal observers; panel D: number of samples in amblyopic observers. The following abbreviations have been used; LSF: low spatial frequency, MSF: medium spatial frequency, HSF: high spatial frequency, FFE: fellow fixing eye, AME: amblyopic eye.

of samples found for amblyopic and fellow fixing eyes. In the constant radius condition, our data showed that increasing the number of elements and the density of the texture has little effect on the magnitude of the internal noise (Fig. 8A), but it did increase the number of

samples (Fig. 8D). In the constant numerosity condition, as the radius increased and the density decreased, the internal noise decreased (Fig. 8B) but the number of samples did not show a consistent pattern (Fig. 8E). In the constant density condition, as the number of

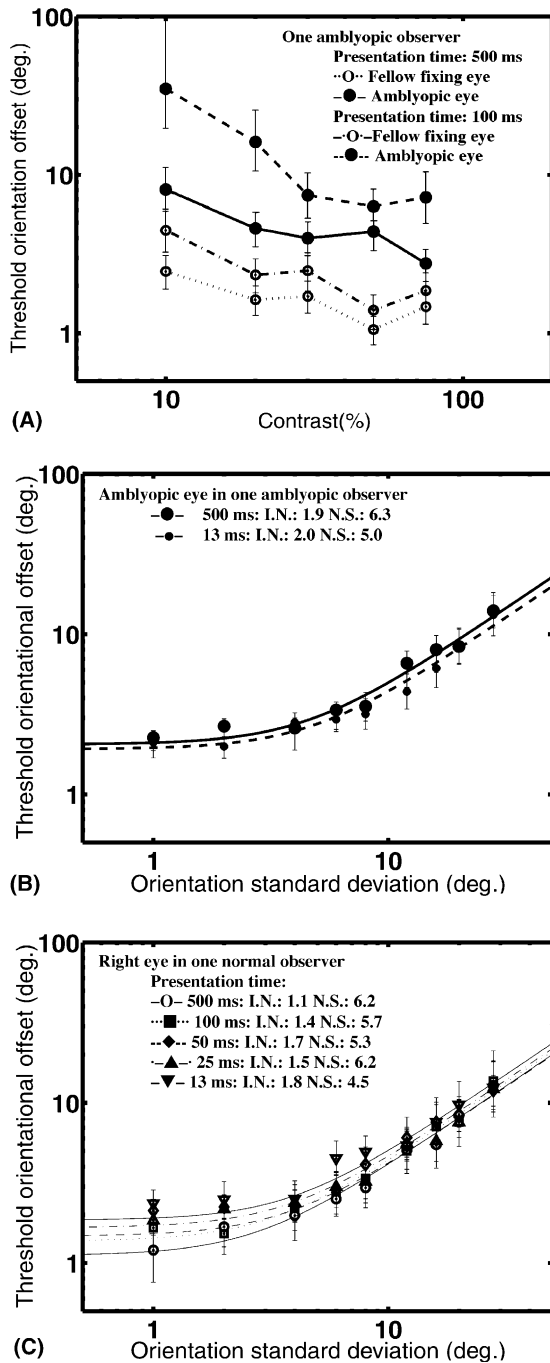


Fig. 7. Mean orientation thresholds for different exposure durations. In (A), orientation discrimination thresholds are plotted for a single Gabor element for the amblyopic and fellow fixing eyes of a strabismic amblyope (BB) for two exposure durations (100 and 500 ms). The amblyopic eye is disadvantaged when the exposure duration is short and this necessitates a different correction factor to bring the performance of amblyopic and fellow fixing eyes together for the single element case. In (B), mean orientation thresholds are plotted against orientation discrimination standard deviation for an amblyopic observer (MA). Orientation integration is not significantly different for two exposure durations (500 and 13 ms). In (C), orientation integration is seen to be invariant with exposure duration for the dominant eye of a normal observer (BM). The parameters of this fit, internal noise (IN) and number of samples (NS) are shown in the inset. The error bars represent 95% confidence intervals.

Table 3

Internal noise and number of samples in one normal and four amblyopic observers in 13 ms presentation time condition

Observers	Internal noise		Number of samples	
	FFE	AME	FFE	AMB
MA	5.00	2.5	2.28	4.85
PH	2.60	2.91	6.92	9.24
RB	3.56	3.26	1.75	2.55
MM	2.79	4.60	2.00	2.40
BB	5.01	5.95	1.30	0.95
BM (normal)	DE 1.47	NDE 1.75	DE 5.42	NDE 4.54

The following abbreviations have been used; FFE: fellow fixing eye, AME: amblyopic eye, DE: dominant eye, NDE: non-dominant eye.

elements and the radius increased, the internal noise decreased (Fig. 8C) and the number of samples increased (Fig. 8F).

These results highlight the importance of numerosity for this task. Unlike density or stimulus extent, the numerosity appears to determine how many samples are taken, a result consistent with the previous work of Dakin (2001) and Allen, Hess, Mansouri, and Dakin (2003). We find this also to be the case for amblyopic and fellow fixing eyes. An interesting difference between results for amblyopic and fellow fixing eyes of the amblyopic observers in our experiment and normal eyes of normal observers in the previous work (Dakin, 2001) concerns the internal noise. Dakin showed that in normals, internal noise varied with density. We found in our amblyopic observers that it varied inversely with the stimulus extent, although the results are not definite.

5. Discussion

The main finding of our study is that amblyopic observers can integrate local orientation information that occurs within different regions of their visual field just as efficiently as normals. This finding is robust across a number of stimulus parameters including exposure duration, numerosity, density and stimulus extent. At the level at which this integration takes place, we find no evidence of either a grossly elevated internal noise or a reduced number of samples. The amblyopic cortex processes these stimuli with the same efficiency as that of the normal cortex or indeed the cortex driven by the fellow fixing eye.

Previous research has highlighted a number of processing deficits in amblyopia, these include, contrast sensitivity, positional uncertainty (Hess & Holliday, 1992; Levi & Klein, 1985), global motion (Simmers et al., 2003), global form (Simmers et al., forthcoming) and orientation (Barrett et al., 2003; Popple & Levi, 2000). How do the present results relate to these deficits? Our method of equating performance in terms of the discrimination of a single Gabor element by manipulating

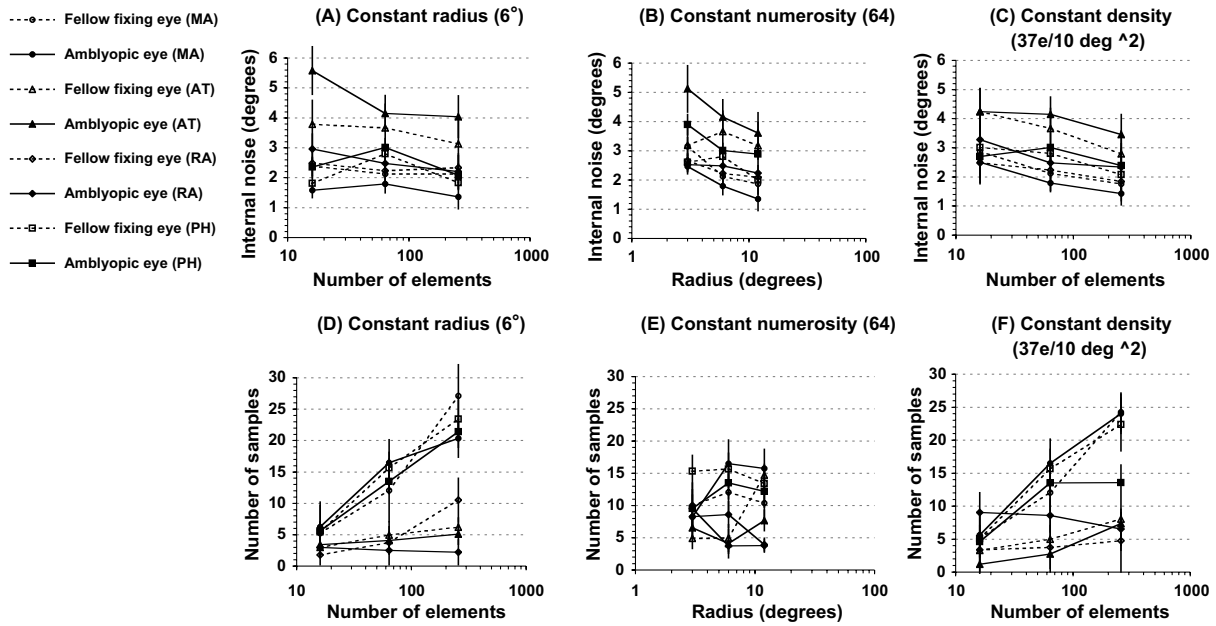


Fig. 8. Effects of various number of elements, presentation area and density on the internal noise and sampling efficiency. In (A) and (D), internal noise and number of samples estimates are compared for the amblyopic and fellow fixing eyes for the fixed radius condition (density and numerosity co-vary). In (B) and (E), internal noise and number of samples estimates are compared for the amblyopic and fellow fixing eyes for the fixed numerosity condition (density and numerosity co-vary). In (C) and (F), internal noise and number of samples estimates are compared for the amblyopic and fellow fixing eyes for the fixed density condition (radius and numerosity co-vary). The error bars represent 95% confidence intervals.

the contrast of the stimuli presented to the fellow fixing eye had the effect of factoring out any downstream influence due to differences in contrast sensitivity or local orientation processing between the parts of the visual system driven by fellow fixing and amblyopic eyes. Furthermore, the fact that the local position of the Gabor elements within the array was irrelevant to the task meant that any positional uncertainty that might be present at the level of the integration process studied here would not influence performance. Thus, the present results are not inconsistent with what we already know about the amblyopic deficit. They are relevant to the findings with a similar task requiring integration of motion where deficits were revealed for amblyopic observers (Simmers et al., 2003). Our finding that local static signals can be integrated with normal efficiency in amblyopia argues that the deficit in amblyopia does not involve integration in general but certain types of integration in particular. It is unlikely however that a common mechanism would determine both the integration of static oriented signals and the direction of moving signals. From the little we know of the physiology, the former would take place within the ventral stream and the latter within the dorsal stream (Mishkin & Ungerleider, 1982). Thus in terms of global integration of visual information, the dorsal stream may be more disadvantaged in amblyopia when it comes to processes involving global integration. Although it should be kept in mind that such deficits might be highly task specific.

5.1. Special forms of orientation integration

The present findings may be relevant to why amblyopes have similar performance to normals when detecting textures based on orientational contrast (Mussap & Levi, 1999). Such texture discriminations however, in principle, can be accomplished by local processes involving orientation discrimination at the edge of the texture-defined region. The present findings are consistent with the conclusions of two earlier studies concerning special forms of orientation integration, in which the encoding of spatial position is a key factor, namely contour integration (Hess et al., 1997) and global shape discrimination (Hess et al., 1999). Amblyopes may be anomalous at these special forms of orientation integration not because their integration of orientation signals per se is necessarily anomalous but because of poor positional encoding (Demanins & Hess, 1996b; Hess & Holliday, 1992; Levi & Klein, 1985).

5.2. Explanations for amblyopia

There are three competing explanations for the neural nature of the underlying anomaly in amblyopia; loss of cells (Levi & Klein, 1986), disarray of cells (Hess, Campbell, & Greenhalgh, 1978) or anomalous interaction between cells (Hess, Campbell, & Zimmern, 1980; Polat, Sagi, & Norcia, 1997). Although there is no reason to expect that these explanations are mutually exclusive,

let us for simplicity consider that they are. The above explanations are sufficiently vague that it is difficult to know to what extent the present results support or refute them. Some general comments can be made but it should be kept in mind that they relate specifically to the type of model used here to fit the data.

5.3. Loss of cells

Our measure of the number of samples comes from the statistical nature of the task. It does not, therefore, relate simply to the number of neural samples taken by the amblyopic visual system. It is really a general measure of efficiency. If there were fewer samples taken by the amblyopic visual system at any point up to the site where orientation integration takes place, one would expect to see a reduction in our “number of samples” measure.

5.4. Disarray of cells

Since the individual Gabors within our arrays were randomly positioned, any purely *positional* disarray involving cells with orientation tuning would not be expected to affect the type of integration we report here. If the positional disarray were at the input stage (i.e. involving the lay-out of the non-oriented sub-units) to cells with orientation tuning, one might expect an anomaly to local orientation processing which in our case is corrected for in our initial equating experiment. If the disarray occurs within the orientation domain, one would expect to see an elevated level of internal noise, which we did observe, but it was of small magnitude and restricted to high spatial frequencies.

5.5. Anomalous interactions between cells

We found that the efficiency of integration in amblyopia did not depend on the spatial arrangement of the local oriented signals (numerosity, density or spatial extent). A particularly revealing case is where multiple elements are used but integration is not required (i.e. where the distribution $SD = 0$; see Fig. 3B). In this case, at high spatial frequencies where we show the integration of orientation is defective in amblyopic eyes, performance in the case where the standard deviation was zero, is not significantly different between normal and amblyopic eyes. This suggests that there were no detrimental effects in the multi-element case per se due to lateral interactions. We can therefore rule out anomalous lateral interactions of the most general form occurring before the site of integration for the type of integration measured here. However, our results do not bear on some more specific types of anomalies between neighbouring elements that does not affect their later integration.

Acknowledgment

This work was supported by a Canadian Institute for Health Research (CIHR) grant (MOP 108-18) to Robert F. Hess.

References

- Ahumada, A. J., Jr., & Watson, A. B. (1985). Equivalent-noise model for contrast detection and discrimination. *Journal of Optical Society of America A: Optics, Image Sciences, and Vision*, 2(7), 1133–1139.
- Allen, H. A., Hess, R. F., Mansouri, B., & Dakin, S. C. (2003). Integration of first- and second-order orientation. *Journal of Optical Society of America A: Optics, Image Sciences, and Vision*, 20(6), 974–986.
- Baker, C. L. J., Hess, R. F., & Zihl, J. (1991). Residual motion perception in a “motion-blind” patient, assessed with limited-lifetime random dot stimuli. *Journal of Neuroscience*, 11(2), 454–461.
- Barlow, H. B. (1957). Increment thresholds at low intensities considered as signal/noise discriminations. *Journal of Physiology*, 136(3), 469–488.
- Barrett, B. T., Pacey, I. E., Bradley, A., Thibos, L. N., & Morrill, P. (2003). Nonveridical visual perception in human amblyopia. *Investigative Ophthalmology and Visual Sciences*, 44(4), 1555–1567.
- Bradley, A., & Skottun, B. C. (1984). The effects of large orientation and spatial frequency differences on spatial discriminations. *Vision Research*, 24(12), 1889–1896.
- Brainard, D. H. (1997). The psychophysics toolbox. *Spatial Vision*, 10(4), 433–436.
- Britten, K. H., Shadlen, M. N., Newsome, W. T., & Movshon, J. A. (1992). The analysis of visual motion: a comparison of neuronal and psychophysical performance. *Journal of Neuroscience*, 12(12), 4745–4765.
- Britten, K. H., Shadlen, M. N., Newsome, W. T., & Movshon, J. A. (1993). Responses of neurons in macaque MT to stochastic motion signals. *Visual Neuroscience*, 10(6), 1157–1169.
- Caelli, T., Brettel, H., Rentschler, I., & Hilz, R. (1983). Discrimination thresholds in the two-dimensional spatial frequency domain. *Vision Research*, 23(2), 129–133.
- Crewther, D. P., & Crewther, S. G. (1990). Neural site of strabismic amblyopia in cats: spatial frequency deficit in primary cortical neurons. *Experimental Brain Research*, 79(3), 615–622.
- Dakin, S. C. (2001). Information limit on the spatial integration of local orientation signals. *Journal of Optical Society of America A: Optics, Image Sciences, and Vision*, 18(5), 1016–1026.
- Dakin, S. C., & Watt, R. J. (1994). Detection of bilateral symmetry using spatial filters. *Spatial Vision*, 8(4), 393–413.
- Demanins, R., & Hess, R. F. (1996a). Effect of exposure duration on spatial uncertainty in normal and amblyopic eyes. *Vision Research*, 36(8), 1189–1193.
- Demanins, R., & Hess, R. F. (1996b). Positional loss in strabismic amblyopia: inter-relationship of alignment threshold, bias, spatial scale and eccentricity. *Vision Research*, 36(17), 2771–2794.
- Demanins, R., Hess, R. F., Williams, C. B., & Keeble, D. R. (1999). The orientation discrimination deficit in strabismic amblyopia depends upon stimulus bandwidth. *Vision Research*, 39(24), 4018–4031.
- Eggers, H. M., & Blakemore, C. (1978). Physiological basis of anisometropic amblyopia. *Science*, 201(4352), 264–267.
- Foster, D. H., & Bishop, W. F. (1987). Bootstrap variance estimators for the parameters of small-sample sensory-performance functions. *Biological Cybernetics*, 57(4–5), 341–347.

- Gstalder, R. J. (1971). Laser interferometric acuity in amblyopia. *Journal of Pediatric Ophthalmology*, 8, 251–256.
- Heeley, D. W. (1987). Spatial frequency discrimination for sine wave gratings with random, bandpass frequency modulation: evidence for averaging in spatial acuity. *Spatial Vision*, 2(4), 317–335.
- Heeley, D. W., Buchanan-Smith, H. M., Cromwell, J. A., & Wright, J. S. (1997). The oblique effect in orientation acuity. *Vision Research*, 37(2), 235–242.
- Hess, R. F., & Anderson, S. J. (1993). Motion sensitivity and spatial undersampling in amblyopia. *Vision Research*, 33(7), 881–896.
- Hess, R. F., Bradley, A., & Piotrowski, L. (1983). Contrast-coding in amblyopia. I. Differences in the neural basis of human amblyopia. *Proceeding of the Royal Society of London, Series B: Biological Sciences*, 217(1208), 309–330.
- Hess, R. F., Burr, D. C., & Campbell, F. W. (1980). A preliminary investigation of neural function and dysfunction in amblyopia—III. Co-operative activity of amblyopic channels. *Vision Research*, 20(9), 757–760.
- Hess, R. F., Campbell, F. W., & Greenhalgh, T. (1978). On the nature of the neural abnormality in human amblyopia; neural aberrations and neural sensitivity loss. *Pflugers Archiv—European Journal of Physiology*, 377(3), 201–207.
- Hess, R. F., Campbell, F. W., & Zimmern, R. (1980). Differences in the neural basis of human amblyopias: the effect of mean luminance. *Vision Research*, 20(4), 295–305.
- Hess, R. F., & Dakin, S. C. (1999). Contour integration in the peripheral field. *Vision Research*, 39(5), 947–959.
- Hess, R. F., & Holliday, I. E. (1992). The spatial localization deficit in amblyopia. *Vision Research*, 32(7), 1319–1339.
- Hess, R. F., & Howell, E. R. (1977). The threshold contrast sensitivity function in strabismic amblyopia: evidence for a two type classification. *Vision Research*, 17(9), 1049–1055.
- Hess, R. F., Ledgeway, T., & Dakin, S. (2000). Impoverished second-order input to global linking in human vision. *Vision Research*, 40(24), 3309–3318.
- Hess, R. F., McIlhagga, W., & Field, D. J. (1997). Contour integration in strabismic amblyopia: the sufficiency of an explanation based on positional uncertainty. *Vision Research*, 37(22), 3145–3161.
- Hess, R. F., Wang, Y. Z., Demanins, R., Wilkinson, F., & Wilson, H. R. (1999). A deficit in strabismic amblyopia for global shape detection. *Vision Research*, 39(5), 901–914.
- Hess, R. H., Baker, C. L., Jr., & Zihl, J. (1989). The “motion-blind” patient: low-level spatial and temporal filters. *Journal of Neuroscience*, 9(5), 1628–1640.
- Kiorpes, L., Kiper, D. C., O’Keefe, L. P., Cavanaugh, J. R., & Movshon, J. A. (1998). Neuronal correlates of amblyopia in the visual cortex of macaque monkeys with experimental strabismus and anisometropia. *Journal of Neuroscience*, 18(16), 6411–6424.
- Lawden, M. C., Hess, R. F., & Campbell, F. W. (1982). The discriminability of spatial phase relationships in amblyopia. *Vision Research*, 22(8), 1005–1016.
- Lawwill, T., & Burian, H. M. (1966). Luminance, contrast function and visual acuity in functional amblyopia. *American Journal of Ophthalmology*, 62(3), 511–520.
- Levi, D. M., & Klein, S. A. (1985). Vernier acuity, crowding and amblyopia. *Vision Research*, 25(7), 979–991.
- Levi, D. M., & Klein, S. A. (1986). Sampling in spatial vision. *Nature*, 320(6060), 360–362.
- Levi, M., & Harwerth, R. S. (1977). Spatio-temporal interactions in anisometric and strabismic amblyopia. *Investigative Ophthalmology and Visual Science*, 16(1), 90–95.
- Loshin, D. S., & Jones, R. (1982). Contrast sensitivity as a function of exposure duration in the amblyopic visual system. *American Journal of Optometry and Physiological Optics*, 59(7), 561–567.
- Mishkin, M., & Ungerleider, L. G. (1982). Contribution of striate inputs to the visuospatial functions of parieto-occipital cortex in monkeys. *Behavioural Brain Research*, 6(1), 57–77.
- Morrone, M. C., Burr, D. C., & Vaina, L. M. (1995). Two stages of visual processing for radial and circular motion. *Nature*, 376(6540), 507–509.
- Movshon, J. A., Adelson, E. H., Gizzi, M. S., & Newsome, W. T. (1985). *The analysis of moving visual patterns in Pattern Recognition mechanisms*. Rome: Vatican press, pp. 117–151.
- Movshon, J. A., Eggers, H. M., Gizzi, M. S., Hendrickson, A. E., Kiorpes, L., & Boothe, R. G. (1987). Effects of early unilateral blur on the macaque’s visual system. III. Physiological observations. *Journal of Neuroscience*, 7(5), 1340–1351.
- Mussap, A. J., & Levi, D. M. (1999). Orientation-based texture segmentation in strabismic amblyopia. *Vision Research*, 39(3), 411–418.
- Newsome, W. T., & Pare, E. B. (1988). A selective impairment of motion perception following lesions of the middle temporal visual area (MT). *Journal of Neuroscience*, 8(6), 2201–2211.
- Pardhan, S. (2004). Contrast sensitivity loss with aging: sampling efficiency and equivalent noise at different spatial frequencies. *Journal of Optical Society of America A: Optics, Image Sciences, and Vision*, 21(2), 169–175.
- Pass, A. F., & Levi, D. M. (1982). Spatial processing of complex stimuli in the amblyopic visual system. *Investigative Ophthalmology and Visual Science*, 23(6), 780–786.
- Pelli, D. G. (1997). The VideoToolbox software for visual psychophysics: transforming numbers into movies. *Spatial Vision*, 10(4), 437–442.
- Pelli, D. G., & Zhang, L. (1991). Accurate control of contrast on microcomputer displays. *Vision Research*, 31(7–8), 1337–1350.
- Polat, U., Sagi, D., & Norcia, A. M. (1997). Abnormal long-range spatial interactions in amblyopia. *Vision Research*, 37, 737–744.
- Popple, A. V., & Levi, D. M. (2000). Amblyopes see true alignment where normal observers see illusory tilt. *Proceedings of the National Academy of Sciences of the United States of America*, 97(21), 11667–11672.
- Rentschler, I., & Hilz, R. (1985). Amblyopic processing of positional information. Part I: Vernier acuity. *Experimental Brain Research*, 60(2), 270–278.
- Rizzo, M., Nawrot, M., & Zihl, J. (1995). Motion and shape perception in cerebral akinetopsia. *Brain*, 118(Pt. 5), 1105–1127.
- Rosenbach, O. (1903). Ueber monokulare Vorherrschaft beim binokularen Sehen. *Munchener Medizinische Wochenschrift*, 30, 1290–1292.
- Salzman, C. D., Murasugi, C. M., Britten, K. H., & Newsome, W. T. (1992). Microstimulation in visual area MT: effects on direction discrimination performance. *Journal of Neuroscience*, 12(6), 2331–2355.
- Simmers, A. J., Ledgeway, T., & Hess, R. F. (forthcoming). Separating the influences of visibility and anomalous integration processes on the perception of global spatial form in human amblyopia. *Vision Research*.
- Simmers, A. J., Ledgeway, T., Hess, R. F., & McGraw, P. V. (2003). Deficits to global processing in human amblyopia. *Vision Research*, 43, 729–738.
- Treutwein, B., Rentschler, I., Zetzsche, C., Scheidler, M., & Boergen, K. P. (1996). Amblyopic quasi-blindness for image structure. *Vision Research*, 36(14), 2211–2228.
- Vaina, L. M., Lemay, M., Bienfang, D. C., Choi, A. Y., & Nakayama, K. (1990). Intact “biological motion” and “structure from motion” perception in a patient with impaired motion mechanisms: a case study. *Visual Neuroscience*, 5(4), 353–369.
- Vandenbussche, E., Vogels, R., & Orban, G. A. (1986). Human orientation discrimination: changes with eccentricity in normal and amblyopic vision. *Investigative Ophthalmology and Visual Science*, 27(2), 237–245.
- Watt, R. J., & Andrews, D. (1981). APE. Adaptive Probit estimation of the psychometric function. *Current Psychological Review*, 1, 205–214.

- Watt, R. J., & Hess, R. F. (1987). Spatial information and uncertainty in anisometric amblyopia. *Vision Research*, 27(4), 661–674.
- Watt, R. J., & Morgan, M. J. (1983). The recognition and representation of edge blur: evidence for spatial primitives in human vision. *Vision Research*, 23(12), 1465–1477.
- Weiss, C., Rentschler, I., & Caelli, T. (1985). Amblyopic processing of positional information. Part II: Sensitivity to phase distortion. *Experimental Brain Research*, 60(2), 279–288.
- Wong, E. H., Levi, D. M., & McGraw, P. V. (2001). Is second-order spatial loss in amblyopia explained by the loss of first-order spatial input?. *Vision Research*, 41(23), 2951–2960.
- Zeevi, Y. Y., & Mangoubi, S. S. (1984). Vernier acuity with noisy lines: estimation of relative position uncertainty. *Biological Cybernetics*, 50(5), 371–376.
- Zihl, J., von Cramon, D., & Mai, N. (1983). Selective disturbance of movement vision after bilateral brain damage. *Brain*, 106(Pt. 2), 313–340.